Oscillatory magnetoresistance of gallium*

R. L. Brown and C. B. Friedberg
Physics Department, University of Virginia, Charlottesville, Virginia 22901
(Received 7 July 1976)

We present the results of an experimental investigation of the oscillatory magnetoresistance of gallium. The frequency spectrum of the large-amplitude magnetic-breakdown-generated oscillations for field directions in the bc plane was measured. A particularly rich spectrum which includes five previously unreported frequency components was observed for $\vec{H}$ along the c axis. The results are compared with existing de Haas–van Alphen data as well as with the best available Fermi-surface model due to Reed. We discuss a possible interpretation of the data in terms of the one-dimensional coupled orbit network which emerges from Reed's calculation, but for which the consequences have not been previously considered. The calculation is shown to be only partially consistent with the experimental data.

I. INTRODUCTION

Several previous studies of the galvanomagnetic properties of gallium have contributed greatly to the present partial understanding of the Fermi-surface topology and electronic structure. Reed and Marcus[1] established that gallium is a compensated metal and reported the existence of open trajectories in the k_z direction. More detailed investigations by Kimball and Stark[2] and by Cook and Datars[3,4] revealed the presence of k_x-directed open trajectories as well. Kimball and Stark were able to resolve four distinct angular regions in the bc plane for which the applied magnetic field gives rise to k_x open trajectories, and from measurements of the field dependence of the transverse magnetoresistance, determined that in three of those regions the trajectories are generated by magnetic breakdown.

A great deal more information about the electronic structure of a metal, in addition to the determination of Fermi-surface connectivity and associated semiclassical electron trajectories, can often be obtained from studies of the *oscillatory* magnetoresistance. This is especially true in those cases where magnetic breakdown is important and oscillatory components of the magnetoresistance having amplitudes much larger than the standard de Haas–Shubnikov oscillations are observable. Large-amplitude magnetoresistance oscillations of this type were observed in gallium by Kimball and Stark,[2] but no quantitative study was undertaken.

We present here the results of our detailed investigation of the oscillatory magnetoresistance of gallium. Comparison will be made with previous de Haas–van Alphen (DHVA) data[5,6] and with the recent and more complete DHVA results of Holroyd and Datars.[7] Despite the extensive experimental studies of Ga utilizing a great many of the techniques of Fermiology,[8,9] there has not yet emerged a band-structure and Fermi-surface model which are fully consistent with the data. By far the most successful band-structure calculation to date is the pseudopotential calculation of Reed,[10] and we will examine in detail the areas of consistency and inconsistency between our experimental results and that calculation.

Crystalline gallium forms a base-centered orthorhombic lattice with lattice parameters $a = 4.516$ Å, $b = 4.491$ Å, and $c = 7.633$ Å at 4.2 K.[11] The base centers are located on the (100) face (or bc plane) of the orthorhombic cell. A rhombic primitive cell is defined by taking the vectors to the base centers: $\vec{x}_1 = \vec{a}$, $\vec{x}_2 = \frac{1}{2}\vec{b} + \frac{1}{2}\vec{c}$, and $\vec{x}_3 = -\frac{1}{2}\vec{b} + \frac{1}{2}\vec{c}$. This primitive cell has one-half the volume of the orthorhombic cell and contains four gallium atoms, each of which contributes three conduction electrons. Since the ratio $c/b = 1.700$ is very nearly $\sqrt{3}$, the lattice is almost hexagonal with near sixfold symmetry about the a axis. The Brillouin zone for gallium is thus the "pseudohexagonal" prism shown in Fig. 1. The complexity of the Fermi surface of gallium is apparently a consequence of both the low crystal symmetry and the large number of conduction electrons per prim-

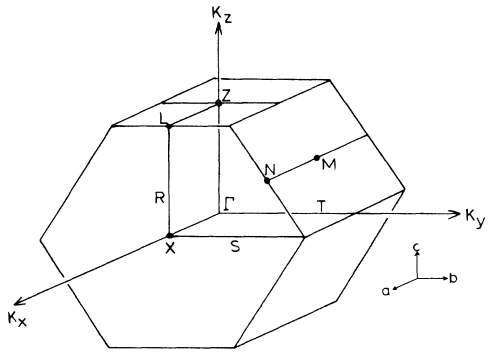

FIG. 1. The pseudohexagonal Brillouin zone for gallium.

itive cell.

Large-amplitude quantum oscillations in the magnetoresistance of various other compensated metals such as Zn,[12] and Mg,[13] have been shown to arise from magnetic breakdown. Several different mechanisms, each involving magnetic breakdown, have been shown to be important and are listed below.

(i) Magnetic breakdown may destroy the volume compensation of hole and electron orbits causing a corresponding transition from large magnetoresistance (H^2 dependence) to small (saturation).[12,13] Oscillatory behavior between these two regimes can result from modulation of the tunneling probabilities (and hence the degree of compensation) by the field-dependent periodic electron density of states on closed orbits involved in magnetic breakdown.[14,15]

(ii) The transition from quadratic to saturating magnetoresistance regimes may also be caused by the existence of magnetic-breakdown-generated open trajectories. Again, oscillatory behavior between the two regimes can result from modulation of the electron transmission probabilities along the open trajectory by the quantized electron density of states on closed orbits coupled to the trajectory.[13]

(iii) Magnetic breakdown may also generate electron interference effects.[16,17] Here the transmission probability of electrons along an open trajectory contains oscillatory components due to the direct interference of phase-coherent electron states on different branches of the trajectory. The frequency of the resulting oscillations does *not* correspond to any closed electron or hole orbit on the Fermi surface, and, as explained elsewhere,[17] the amplitude of such oscillations is unaffected by the temperature broadening of the Fermi distribution and therefore only weakly temperature dependent.

In each of the above cases the magnetoresistance oscillations are generally of larger amplitude than the usual de Haas-Shubnikov oscillations which do not involve magnetic breakdown. The latter result from the oscillatory density of states as manifested in the transport relaxation time, are of small amplitude, and only provide information which is redundant with DHVA data.

II. EXPERIMENTAL PROCEDURE

Single crystals were prepared from high-purity (99.99999%) gallium obtained from Ventron Alfa Products. Typical samples had residual resistivity ratios of 35 000. The crystals were grown from the melt in a lucite mold by the technique described by Yaqub and Cochran[18] and Waldorf.[19] The mold was shaped so as to provide two current and two potential tabs as integral parts of the crystal. The resultant samples were of overall dimensions $\frac{1}{32}\times\frac{1}{32}\times\frac{3}{4}$ in.^{3} The desired crystallographic orientation was achieved by growing from an x-ray aligned seed crystal. In order to obtain good growth from the seed it was necessary to etch the seed with a 3 volume % HCl solution just prior to its insertion in the supercooled molten gallium. After the crystal had solidified it was found that the seed easily detached from the new growth without inducing strain or causing other damage although entire crystal had accepted the seed orientation. Thus a given seed was reusable. The orientations of the seed and samples were determined by comparing Laue back reflection photographs with computer-generated standards.

Magnetoresistance measurements were made with magnetic fields in the range 0–26 kG and temperatures of 1.2–4.2 K. The electromagnet was rotatable in the horizontal place and the entire cryostat and sample could be tilted ±4° in a vertical plane, thus providing two degrees of freedom for accurate *in situ* orientation of the crystal relative to the magnetic field. Final orientation of the samples to within 0.1° was achieved by utilizing the symmetry of magnetoresistance rotation diagrams. The oscillatory magnetoresistance was studied first by preliminary dc detection, and then in detail by the large-amplitude field modulation method.[20] The frequency discrimination feature of this method was essential in analyzing the complex oscillatory spectrum.

Most of the measurements were performed on samples with current axes $\vec{J}$ along the $\vec{b}$ direction. For investigations of the oscillatory spectrum associated with the k_x-directed open-orbit network, the sample axis was mounted horizontally such that the magnetic field could be rotated in the bc plane (longitudinal to transverse configuration). Samples having various other current axes were also utilized for other aspects of the experiment.

III. EXPERIMENTAL RESULTS

The transverse magnetoresistance of Ga for $\vec{J}\parallel\vec{b}$ and $\vec{H}\parallel\vec{c}$ is shown in Fig. 2 for the field range 0–25 kG. Clearly visible on this curve are two large-amplitude oscillatory components with frequencies 0.230 and 0.80 MG, the latter having the greater amplitude. Many other higher-frequency components of sizable amplitude were also observed by means of the field modulation method. Indeed, one such component, 8.7 MG, is also of sufficient amplitude for direct observation in the dc magnetoresistance at only slightly higher fields (see Fig. 8 of Ref. 2).

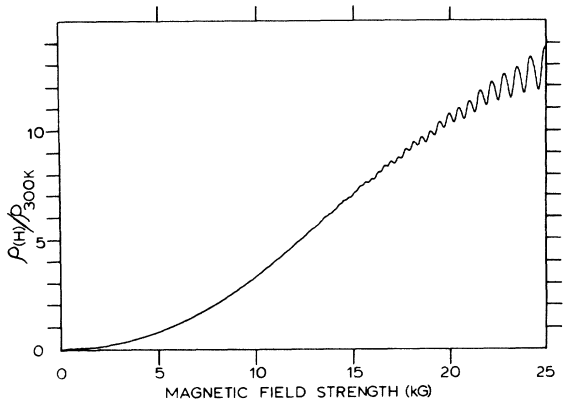

FIG. 2. Transverse magnetoresistance of gallium at 1.6 K for $\vec{H}$ along the c axis and the current $\vec{J}$ along the b axis. The two large amplitude oscillatory components have frequencies 0.230 and 0.80 MG.

A compilation of the frequencies observed for $\vec{H} \| \vec{c}$ is presented in Table I along with a summary of DHVA observations for the same symmetry direction, including the recent results of Holroyd and Datars.[7] Of the ten observed frequencies, five were previously unreported (namely 4.18, 4.39, 33, 44, and 86 MG), although the 4.18-MG frequency was observed simultaneously with this work in the latest DHVA experiments.[7]

The frequency spectrum for $\vec{H}$ along the c axis was the most complex observed and contained the most new information. The frequency branches (frequency versus field direction) corresponding to the new components in the c-axis spectrum were

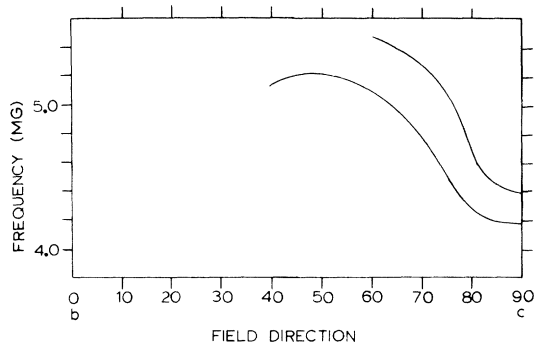

FIG. 3. Frequency branches in the bc plane for two new oscillatory components observed in the magnetoresistance.

measured in the bc plane. The results for the branches corresponding to the 4.18- and 4.39-MG frequencies at $\vec{c}$ are shown in Fig. 3. The lower branch cuts off sharply at 52.5° from the c axis ($\theta = 37.5°$ in the figure), but the upper branch was observed only to about 30° from $\vec{c}$. It should be noted that both components have sizable amplitudes all along the respective branches. A typical data trace for these components is shown in Fig. 4; the dominant frequency results from the lower branch, and the strong beat amplitude from the upper. Branches corresponding to the 33- and 44-MG frequencies were observed in the bc plane to 20° from $\vec{c}$, and the 86 MG was not observed beyond 1.5° from the symmetry axis.

For field directions not in the bc plane, only small-amplitude de Haas–Shubnikov oscillations

TABLE I. Comparison of observed frequencies in the magnetoresistance for $\vec{H} \| \vec{c}$ with the corresponding de Haas–van Alphen data. Frequencies are in MG.

Magnetoresistance (this work)	de Haas–van Alphen		
	Goldstein and Foner[a]	Condon[b]	Holroyd and Datars[c]
		0.0016	
0.203	0.209	~0.20	0.201
0.230	0.232	~0.23	0.223
			0.287
0.80	0.76	0.73	0.790
		1.35	1.363
4.18			4.16
4.39			
8.7	8.5	8.3	8.55
	12.8	12.8	12.5
			13.1
20.7	20.6		20.8
			22.4
33			
44			
86			

[a] Reference 6.
[b] References 5 and 10.
[c] Reference 7.

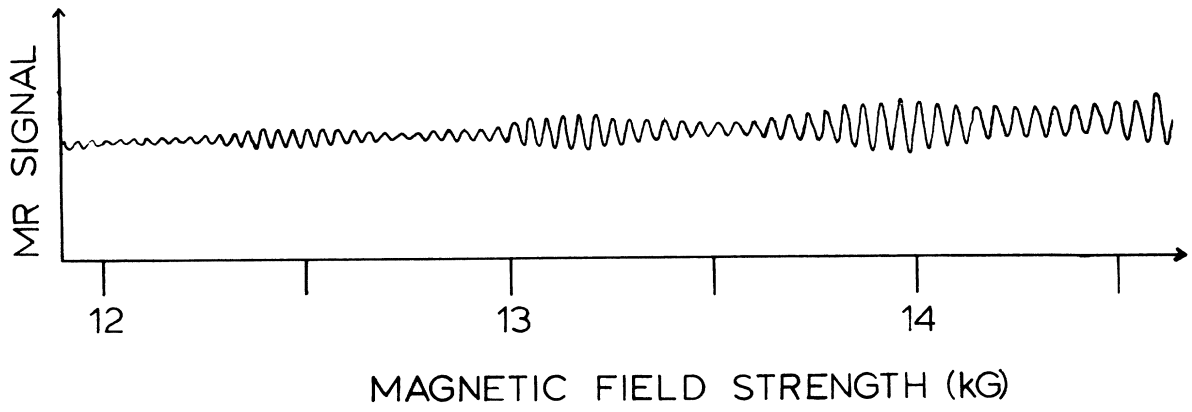

FIG. 4. Magnetoresistance signal (in arbitrary units) as obtained by the field modulation method at 1.4 K for $\vec{H}$ along the c axis. The dominant component has frequency 4.18 MG. The strong beat amplitude results from a 4.39-MG component.

were present in the magnetoresistance. All the observed frequencies were in agreement with published DHVA spectra and so will not be reproduced here. In particular, no new information was obtained from an a-axis current sample despite the importance of the k_z open trajectory in the transverse magnetoresistance when $\vec{H} \parallel \vec{b}$. This supports the previous result that the k_z open trajectory is *not* involved in magnetic breakdown.

A brief experimental search was also undertaken in the DHVA spectrum for the presence of the specific new frequencies in Table I for $\vec{H} \parallel \vec{c}$. No evidence for the higher frequencies (33, 44, and 86 MG) was obtained. The 4.18-MG component was observable, but with considerably smaller amplitude than in the magnetoresistance. However, the strong beat envelope present in the magnetoresistance and resulting from the 4.39-MG component was completely absent in the DHVA spectrum. These results are consistent with the DHVA data of Holroyd and Datars.[7]

A possible source of the oscillatory magnetoresistance components which do not appear in DHVA data is the electron interference mechanism similar to that observed in Mg.[16,17] To test this possibility we investigated the temperature dependence of the amplitudes of these components in the range 1.2–4.2 K. It was found that for $\vec{H} \parallel \vec{c}$ all ten frequency components had temperature-*dependent* amplitudes characterized in the usual way by effective masses m^*. For example, effective masses of the order $0.2m_0$ were measured for both the 86- and 33-MG frequencies, and $0.1m_0$ for the 20.7-, 4.39-, and 4.18-MG frequencies. These compare with effective masses of $(0.15 \pm 0.02)m_0$ and $(0.070 \pm 0.005)m_0$ for the low frequencies, 0.80 and 0.230 MG, respectively.

IV. COMPARISON TO CALCULATED BAND STRUCTURE

As stated earlier, the local pseudopotential calculation by Reed[10] has provided the most successful Fermi-surface model for Ga to date. In this section we will discuss our experimental data in terms of that model and point out both the successes and failures of the model. It should be remembered that the calculation is semiempirical in that the form factors were optimized to provide the observed k_z and k_x open trajectories, and to fit one particular cross section (that of the 7th band electron sheet, or butterfly orbit, at L) from rf size-effect data.[21] However, no adjustments were made to fit the large body of existing DHVA data. For a detailed description of the entire Fermi-surface model we refer the reader to Reed's original paper. We will discuss here only those aspects of the model which are directly relevant to this experiment.

The three Fermi-surface pieces of greatest interest here are the large, multiply connected 6th band hole sheet (6h monster in Reed's nomenclature), the 7th band electron sheet on the T symmetry line (7e saucer), and the 5th band hole sheet (5h ellipsoid) at the symmetry point X. The calculated cross sections of these three pieces in the $k_z = 0$ (central) plane of the Brillouin zone are shown in Fig. 5 in the repeated zone scheme. The 5h and 6h sheets are separated by only small spin-orbit gaps near X (on the S symmetry line) where the 6h piece has a neck. Magnetic breakdown can occur at these gaps, and we will denote the magnetic-breakdown junctions of this type as J_1 junctions. Also shown in Fig. 5 are locations of the 7e saucers at the tips of the monster arms. These two pieces (6h and 7e) are also separated by small

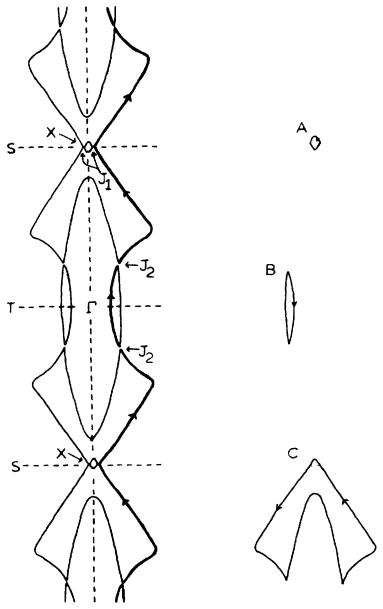

FIG. 5. Cross section in the $k_z = 0$ plane of those sheets of the Fermi surface proposed by Reed which form a one-dimensional coupled-orbit network. Magnetic breakdown can occur at junctions J_1 and J_2 as discussed in the text. The k_x-directed open trajectory generated by breakdown between the 6th and 7th band sheets is denoted by the bold line. Also shown separately are three closed orbits on the network: the 5th band hole ellipsoid (A), the 7th band electron "saucer" (B), and the "single monster" (C) which results from magnetic breakdown between the 5th and 6th band hole sheets.

gaps, and we will refer to the resulting junctions as J_2 junctions.

It should first be noted that the k_x open trajectory, highlighted by the bold face segments and arrows in the figure, results from magnetic breakdown (tunneling) at the J_2-type junctions. Furthermore, the electron trajectories in Fig. 5 form a one-dimensional network of coupled orbits along k_x, and this network supports a large number of distinct closed orbits. Although an important feature of Reed's model is the existence of this fairly complex orbit network, only a few of the simplest orbits have been considered by other workers in analyzing DHVA and other data.

The three orbits of smallest extremal area on the network have indeed been discussed previously and are also depicted in Fig. 5. These are the hole orbit (A) on the 5th band ellipsoid, the electron orbit (B) on the 7th band saucer, and the hole orbit (C) resulting from magnetic breakdown between the 5th and 6th bands at two J_1 junctions. This latter breakdown orbit is commonly called the "single monster" orbit. The predicted frequencies of these orbits from Reed's calculation are 0.07,[22] 0.843, and 10.9 MG, respectively. Since these orbits are all coupled to the open trajectory in Fig. 5 by magnetic breakdown, an additional consequence of this model is the presence of large-amplitude oscillatory components with these frequencies in the magnetoresistance when $\vec{H} \parallel \vec{c}$ and $\vec{J} \parallel \vec{b}$. Assignments of various frequencies in Table I to these orbits have been suggested by Reed.[10] We concur with his assignments of the 0.80- and 8.7-MG frequencies to orbits B and C. However, his tentative assignment of a very low frequency (0.0016 MG) observed by Condon[5] in DHVA measurements is a much poorer fit to orbit A (ellipsoid) than is the 0.230-MG frequency in Table I. Other workers[7,9] have also assigned the 0.230-MG frequency to this piece, and we believe that the experimental observation of this frequency as a large-amplitude component in the magnetoresistance clearly favors this assignment. For completeness we note that an alternative assignment to orbit C of the 12.7-MG DHVA frequency has also been suggested.[7] However, since this frequency is not observed in the magnetoresistance, this assignment is much less likely than the 8.7 MG.

To assign our higher frequencies (in Table I) it is necessary to examine some of the more complex orbits on the network, a subset of which is shown in Fig. 6. Orbit H is the so called "double monster" hole orbit.[10] Orbits A, B (Fig. 5), and H are the only orbits possible on the network in the low-field limit; electrons completing these orbits must undergo Bragg reflection at each junction encountered. All of the other orbits in Fig. 6 are magnetic-breakdown orbits and consist of segments of the electron trajectories on the 5th, 6th, and 7th band sheets coupled together in a variety of ways. The only orbits which exist in the high-field limit are the electron orbit D and the hole orbit K for which the electrons tunnel at each junction encountered. The remaining orbits in Fig. 6 (C, E, F, G, I, J, and L) involve both tunneling and Bragg reflection at the appropriate junctions and exist for intermediate field strengths.

It is apparent from Figs. 5 and 6 that the geometry of this orbit network implies simple algebraic relations between the frequencies of the various orbits. In particular, if the frequencies of orbits A, B, C, and D are specified, all the others are determined. For example, orbit G has frequency $G = 2C - B$. Similar expressions for the other orbits are listed in Table II. Note that these algebraic relations are independent of the detailed shapes of the Fermi-surface pieces and result only from the overall structure of the network. The frequencies calculated by Reed[10] for the orbits in Figs. 5 and 6 are given in Table II. The value of 20 MG for the D orbit was deter-

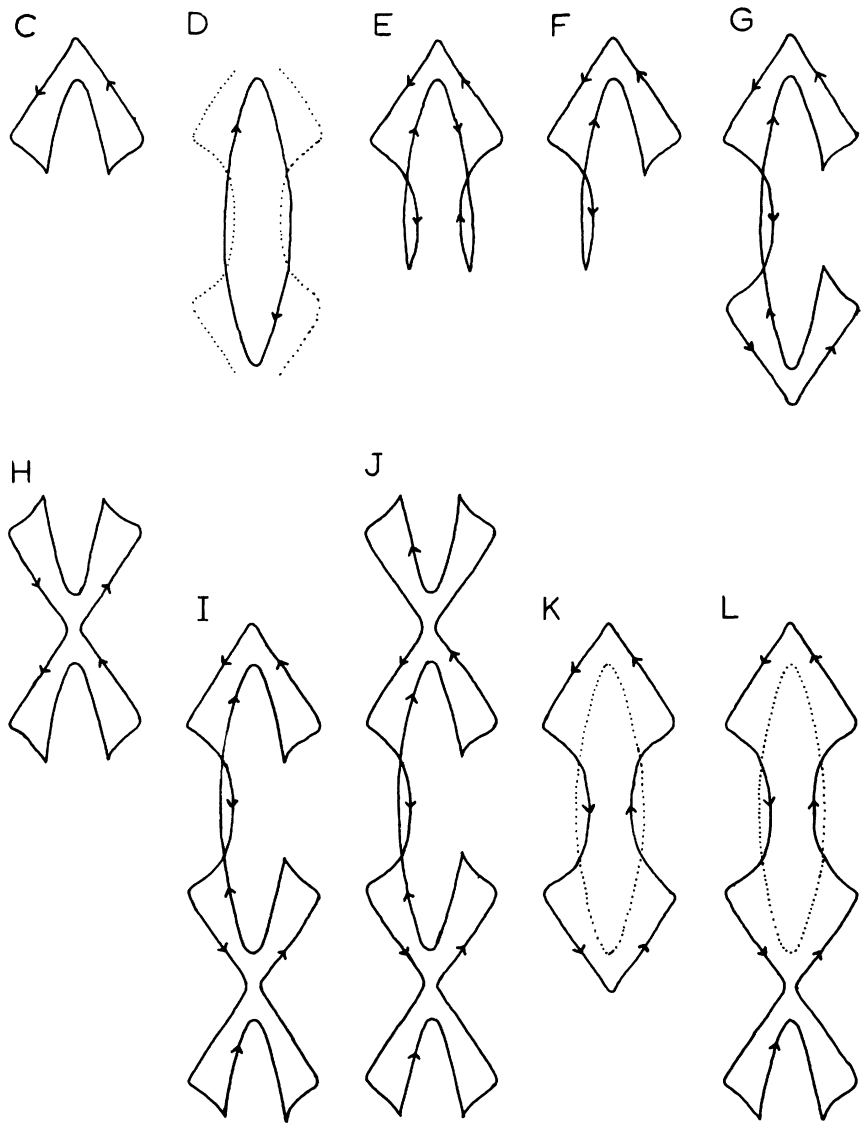

FIG. 6. Some possible orbits on the coupled-orbit network of Reed's model. Electron orbit D and hole orbit K result in the high-field limit when magnetic breakdown is complete. The dotted lines indicate the positions of the orbits on the network.

mined with a planimeter from drawings supplied by Reed and is accurate to only two figures, as are frequencies K and L which are derived from D. The best assignment of the observed frequencies in Table I to the D breakdown orbit is the 20.7-MG component which has also been observed in DHVA experiments. An earlier assignment of this frequency to the 7*e* butterfly orbit at L was proposed by Reed.[10] However, the recent DHVA results have placed a 22.4-MG frequency on the butterfly. Since the 22.4-MG component is *not* observed in the magnetoresistance, it does not result from an orbit on the central breakdown network, whereas just the opposite is true for the 20.7-MG component. We therefore concur with the new assignment of the 22.4 MG to the butterfly.

Assuming that the above assignments of the observed 0.230-, 0.80-, 8.7-, and 20.7-MG frequencies to the A, B, C, and D orbits are correct, we can now predict the actual frequencies of all other orbits on the network by applying the algebraic relations discussed above to these *experimentally determined* frequencies. These results are also presented in Table II in the column labeled "predicted frequencies — Reed's model, modified." We note that there are two possible orbits (J and K) to which the observed 33-MG frequency may be assigned, and one (L) to which the 44 MG may be assigned. Numerous other frequencies, including E, F, G, H, and I, have no counterpart in the experimental data in Table I.

We must now consider the magnetic-breakdown amplitude factors for each orbit to determine which are likely to be observed experimentally.

TABLE II. Frequencies and amplitude factors for coupled orbits shown in Figs. 5 and 6.

Orbit designation	Algebraic frequency relationship	Predicted frequency (MG) Reed's model	Reed's model, modified [a]	Magnetic-breakdown amplitude factor
A	···	0.07	(0.230)	q_1^2
B	···	0.843	(0.80)	q_2^2
C	···	10.9	(8.7)	$p_1^2 q_2^2$
D	···	20	(20.7)	p_2^4
E	$C-2B$	9.2	7.1	$p_1^2 p_2^4 q_2^2$
F	$C-B$	10.1	7.9	$p_1^2 p_2^2 q_2^2$
G	$2C-B$	21.0	16.6	$p_1^4 p_2^4 q_2^2$
H	$2C-A$	21.7	17.2	$q_1^2 q_2^4$
I	$3C-B-A$	31.8	25.1	$p_1^2 q_1^2 p_2^4 q_2^4$
J	$4C-B-2A$	42.6	33.5	$q_1^4 p_2^4 q_2^6$
K	$D+2C-2B$	40	36.5	$p_1^4 p_2^4$
L	$D+3C-2B-A$	51	45.0	$p_1^2 q_1^2 p_2^4 q_2^2$

[a] Experimental values are assigned for orbits A, B, C, and D. The algebraic relationships from Reed's model are then used to calculate the remaining frequencies.

We will denote the probability amplitude for tunneling at a J_i-type junction as p_i $(i=1,2)$, and the corresponding probability amplitude for Bragg reflection as q_i, so that

$$q_i = (1-p_i^2)^{1/2} \tag{1}$$

and

$$p_i^2 = \exp(-H_i/H)\,, \tag{2}$$

where H_i is the relevant magnetic-breakdown parameter. The amplitude for each orbit on the network contains a factor due to magnetic breakdown which is the product of the appropriate p_i and q_i. These factors are given in Table II.

Although the energy gaps and breakdown parameters H_1 and H_2 are not known, some qualitative information is available from the experimental data. The k_x open trajectory shown in Fig. 5 requires tunneling at many successive J_2 junctions, and so the reported experimental evidence for this trajectory[2-4] implies that the breakdown probability is reasonably large at the J_2 junctions for the fields attained in this experiment (26 kG). Thus q_2 is probably small, but not vanishingly so, since orbit B is also observed at 26 kG. Hence we will assume that $p_2 > q_2$, and orbits involving many factors of q_2 will have unobservably small amplitudes, whereas those not involving q_2 (such as orbit D) will be observed. For example, orbit H, the "double monster," involves Bragg reflection at each of four J_2 junctions, and the expected frequency 17.2 MG has not been observed experimentally. Similar effects have been reported in other metals; in Mg, the two-dimensional coupled-orbit network for $\vec{H} \parallel \vec{c}$ contains a hexagonal hole orbit requiring six successive Bragg reflections. This orbit is also not observed due to its small amplitude relative to other coupled orbits on the network.[13]

We will therefore adopt a rough criterion that orbits involving more than two Bragg reflections at J_2 junctions are not observable due to the small Bragg reflection probabilities. This assumption eliminates orbits H, I, and J from consideration. Of the remaining orbits, the total breakdown orbits D and K contain no factors q_2 and should have reasonably large amplitudes. The observed 20.7-MG frequency has been assigned to D, and it is possible that the 33 MG results from K, although the agreement with the predicted frequency (36.5 MG) is much less convincing. A viable orbit for the observed 44-MG frequency is orbit L having a predicted frequency of 45.0 MG and having only two factors of q_2 in the amplitude, as do other observed orbits such as B and C. Thus several of the observed frequencies have reasonable assignments on the coupled-orbit network. However, the criterion stated above also implies that orbits E, F, and G in Fig. 6 which also require only two Bragg reflections at the J_2 junctions should be observed, but no frequencies near the predicted 7.1, 7.9, or 16.6 MG are observed experimentally.

A further and more serious inconsistency in Reed's model is the lack of an explanation for the observed 86-MG frequency for $\vec{H}$ along $\vec{c}$. A large coupled orbit traversing three zones, having a

predicted frequency of 89 MG, and satisfying the above criterion at the J_2 junctions can indeed be constructed on the network. However, on the basis of the measured effective masses for the smaller orbits from which it would be comprised, one would expect a large effective mass ($m^* > 1.0m_0$) for this orbit. Since the measured effective mass for the 86-MG component is only $\sim 0.2m_0$, we believe that such an identification would be incorrect. We also note that there are no appropriate trajectories on the network which by the interference mechanism could give rise to an 86-MG oscillatory component having a weakly temperature-dependent amplitude.

Finally, it is clear that the two frequency branches in Fig. 3 have no possible assignments on this network. Holroyd and Datars[7] have assigned the lower branch to the 8th band electron ellipsoid at L (not in the $k_z=0$ plane) for which Reed's calculation gives 3.94 MG for $\vec{H}$ along $\vec{c}$. The agreement with the observed value (4.18 MG) is excellent and we concur with this assignment. However, it is only possible to assign one frequency branch in this range, and no other assignment for the 4.39-MG branch is possible on Reed's Fermi-surface model.

V. CONCLUSIONS

We have found that the best calculated Fermi surface for gallium is only partially consistent with the experimental data. Several important features of the model appear to be correct. First, in addition to the k_x open trajectory (an initial constraint), the calculation predicts the existence in the $k_z=0$ plane of a one-dimensional coupled-orbit network generated by magnetic breakdown. The observed complex spectrum of large-amplitude oscillations in the magnetoresistance for $\vec{H} \parallel \vec{c}$ and $\vec{J} \parallel \vec{b}$ is strong evidence for such a network. Second, we have had limited success in assigning various components of the observed frequency spectrum (0.230, 0.80, 8.7, 20.7, 33, and 44 MG) to orbits on the network, where the three higher frequencies result from magnetic-breakdown orbits not previously considered.

The same assumptions invoked in these assignments, however, also lead to predictions of various other lower-frequency components in the range 7–17 MG which are not observed experimentally. Also, in the proposed interpretation, the model provides no Fermi-surface orbits for either the 4.39-MG branch reported here in the magnetoresistance, or the 0.0016-MG DHVA component reported by Condon. A far more serious inconsistency in the model is its failure to provide the very-high-frequency component (86 MG) with effective mass $m^* \sim 0.2m_0$ which is observed in the magnetoresistance for $\vec{H} \parallel \vec{c}$. Thus there remain several major difficulties in Reed's pseudopotential calculation. A more sophisticated empirical calculation which fully utilizes both this new magnetoresistance data and the recent DHVA data of Holroyd and Datars would be most welcome at this time.

Note added in proof. R. W. Stark and R. Reifenberger have shown that interference oscillations are characterized by small *nonzero* effective masses in the general case where the transit times for electrons on the two interference trajectories are unequal. Although this does not alter our conclusions regarding Reed's model, it is possible that interference effects are indeed the source of the 86-MG component and must certainly be considered in developing a model which is fully consistent with the data.

ACKNOWLEDGMENTS

We are indebted to W. R. Datars and F. W. Holroyd for sending their de Haas–van Alphen results prior to publication, and to W. A. Reed for supplying the detailed cross sections of the gallium Fermi surface from his pseudopotential calculation.

---

*Supported in part by USERDA, contract No. AT(40-1)-3105.

[1]W. A. Reed and J. A. Marcus, Phys. Rev. 126, 1298 (1962).
[2]J. C. Kimball and R. W. Stark, Phys. Rev. B 4, 1786 (1971).
[3]J. R. Cook and W. R. Datars, Phys. Rev. B 1, 1415 (1970).
[4]J. R. Cook and W. R. Datars, Can. J. Phys. 48, 3021 (1970).
[5]J. H. Condon, Bull. Am. Phys. Soc. 9, 239 (1964). See also the appendix of Ref. 10.
[6]A. Goldstein and S. Foner, Phys. Rev. 146, 442 (1966).
[7]F. W. Holroyd and W. R. Datars (private communication).
[8]A full bibliography of gallium studies prior to 1969 is given in Ref. 10.
[9]R. Griessen, H. Krugmann, and H. R. Ott, Phys. Rev. B 10, 1160 (1974).
[10]W. A. Reed, Phys. Rev. 188, 1184 (1969).
[11]C. S. Barrett, in *Advances in X-Ray Analysis*, edited by W. M. Mueller (Plenum, New York, 1962), Vol. 5.
[12]R. W. Stark, Phys. Rev. 135, A1698 (1964).
[13]R. W. Stark and L. M. Falicov, in *Progress in Low Temperature Physics*, edited by C. J. Gorter (North-Holland, Amsterdam, 1967), Vol. V.

[14]L. M. Falicov, A. B. Pippard, and P. R. Sievert, Phys. Rev. 151, 498 (1966).
[15]For a review see A. B. Pippard, in *The Physics of Metals*, edited by J. M. Ziman (Cambridge U. P., Cambridge, 1969), Vol. 1.
[16]R. W. Stark and C. B. Friedberg, Phys. Rev. Lett. 26, 556 (1971).
[17]R. W. Stark and C. B. Friedberg, J. Low Temp. Phys. 14, 111 (1974).
[18]M. Yaqub and J. F. Cochran, Phys. Rev. 137, 1182 (1965).
[19]D. Waldorf, Cryogenics 8, 244 (1968).
[20]R. W. Stark and L. R. Windmiller, Cryogenics 8, 272 (1968).
[21]A. Fukumoto and M. W. P. Strandberg, Phys. Rev. 155, 685 (1967).
[22]The frequency for the 5*h* ellipsoid was calculated by the authors from the cross sections provided them by W. A. Reed.